Wave Propagation in Periodic Composites: Higher-Order Asymptotic Analysis Versus Plane-Wave Expansions Method

I. V. Andrianov
Institut für Allgemeine Mechanik,
RWTH Aachen University,
Templergraben 64,
D-52056 Aachen, Germany
e-mail: igor_andrianov@inbox.ru

J. Awrejcewicz
Department of Automatics and Biomechanics,
Technical University of Łódź,
1/15 Stefanowski Street,
90-924 Łódź, Poland
e-mail: awrejcew@p.lodz.pl

V. V. Danishevs'kyy
Prydniprovs'ka State Academy of Civil
Engineering and Architecture,
24a Chernishevskogo Street,
49600 Dnipropetrovs'k, Ukraine
e-mail: vdanish@ukr.net

D. Weichert
Institut für Allgemeine Mechanik,
RWTH Aachen University,
Templergraben 64,
D-52056 Aachen, Germany
e-mail: weichert@iam.rwth-aachen.de

This work is devoted to a comparison of different methods determining stop-bands in 1D and 2D periodic heterogeneous media. For a 1D case, the well-known dispersion equation is studied via asymptotic approach. In particular, we show how homogenized solutions can be obtained by elementary series used up to any higher-order. We illustrate and discuss a possible application of asymptotic series regarding parameters other than wavelength and frequency. In addition, we study antiplane elastic shear waves propagating in the plane through a spatially infinite periodic composite material consisting of an infinite matrix and a square lattice of circular inclusions. In order to solve the problem, a homogenization method matched with asymptotic solution on the cell with inclusion of the large volume fracture is proposed and successfully applied. First and second approximation terms of the averaging method provide the estimation of the first stop-band. For validity and comparison with other approaches, we have also applied the Fourier method. The Fourier method is shown to work well for relatively small inclusions, i.e., when the inclusion-associated parameters and matrices slightly differ from each other. However, for evidently contrasting structures and for large inclusions, a higher-order homogenization method is advantageous. Therefore, a higher-order homogenization method and the Fourier analysis can be treated as mutually complementary.
[DOI: 10.1115/1.4002389]

Keywords: composite material, wave propagation, homogenization approach, asymptotic methods, dispersion, band gap

1 Introduction

In many cases, the investigation of wave propagating in periodic media can be reduced to the solution of differential equations with periodic coefficients. One of the most popular approximations applied in this challenging field of science is the homogenization approach [1–4]. However, the most interesting phenomenon exhibited by wave propagation in a nonhomogeneous medium is the so-called stop-band effect. Notice that the homogenization approach does not permit this effect to be determined in the first-order approximation of the averaging method. In principle, the second-order approximation of the averaging procedure allows us to arrive at the solution sought, but there is a problem with the accuracy of this approximation.

Let us begin with a study of the problem for the 1D case. In mathematical literature, the study of differential equations with periodic coefficients is known as Floquet theory [5]. In physics, it goes under the name of "Bloch method" since Bloch used that approach in his study of motion of an electron in a crystalline solid [6]. Observe that for a periodic 1D composite consisting of two types of components, the Floquet–Bloch approach allows us to get an exact form of dispersive equation [7]. An asymptotical analysis of that equation allows us to get a few terms of a homogenized solution and enables the application of a higher-order homogenization approach to detect the stop-band effect. Besides, in the 1D case, a possibility to apply asymptotic series regarding parameters other than wavelength and frequency is addressed. The series mentioned may be treated as an alternative to a higher-order homogenization approach.

For 2D composites in the low frequency range, the wave dispersion phenomena can be analyzed by the higher-order asymptotic homogenization method (AHM) [8], the Fourier approach (the so-called plane-wave (PW) expansion method [9–13]), the Rayleigh multipole-expansion method and its generalizations [14], and the Korringa–Kohn–Rostoker method (also known as the multiple scattering method [15]). All these methods represent a solution represented by the infinite series expansions, and their convergence usually depends on the contrast between properties of the components.

The first key idea of using homogenization to study spectral properties of the problems with periodic coefficients, in particular, the Floquet–Bloch spectrum, can be found in Refs. [16,17] (see also further references therein). More recent papers [18–21] are devoted to further theoretical development of the relations between the Floquet–Bloch theory and homogenization. Next, the idea of using the higher-order asymptotic homogenization in a similar context is also partially referred to in literature. Apart from the references mentioned above, see also Ref. [22], where, in particular, the two-scale asymptotic expansion is combined with a variational truncation to derive higher-order homogenized equations in ε (higher-order error bounds were obtained as well).

The applications of asymptotic series regarding parameters other than wavelengths and frequencies are treated in literature rather marginally. For example, in Refs. [23,24], the asymptotics of the Floquet–Bloch spectrum, with ε related not only to the small periodicity but also to the (critically scaled) high contrast,

Contributed by the Design Engineering Division of ASME for publication in the JOURNAL OF COMPUTATIONAL AND NONLINEAR DYNAMICS. Manuscript received May 25, 2009; final manuscript received July 30, 2010; published online October 7, 2010. Assoc. Editor: Lawrie Virgin.

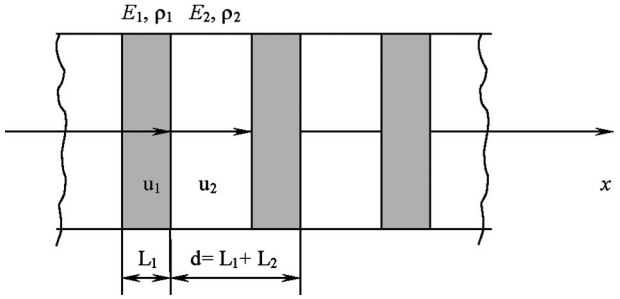

Fig. 1 1D composite material ($L_1+L_2=d$)

are studied. Recent developments include those, for e.g., high contrasts in both stiffness and density [25,26] and for more general high contrast elasticity [27,28].

Elastic and acoustic wave band structures were investigated in the works [11,12] using the plane-wave expansion method. Another widely used approach to study wave propagation in periodic media is the finite difference time domain method (see, for instance, Ref. [29] and references cited therein). A recent review of classical vibration modes in phononic lattices is given in Ref. [13].

In this paper, we study antiplane shear waves in a fiber-reinforced composite material with a square lattice of circular inclusions. In order to solve the problem formulated so far, we apply the homogenization method with an asymptotic solution regarding a cell for large inclusion dimensions. The first and second approximations of the homogenization procedure are obtained, which enables detection of the first stop-band. For comparison and reliability estimation, the problem is solved additionally using the method of Fourier series. It has been shown that the Fourier method yields good results for relatively small inclusion dimensions and when the inclusion parameters and matrices differ slightly from each other. In the case of contrasting structures, the higher-order homogenization method is recommended. Therefore, both methods studied can be treated as mutually complementary.

This paper is organized as follows. In Sec. 2, we describe a dispersion equation for the 1D case. Long-wave asymptotic for the 1D case is obtained in Sec. 3. Asymptotics regarding relative impedance are proposed in Sec. 4. A governing boundary value problem (BVP) for the 2D case is formulated in Sec. 5. Higher-order AHM and PW expansion methods are applied to the 2D problem in Secs. 6 and 7, respectively. Numerical examples are proposed in Sec. 8. Finally, a brief discussion of the obtained results is presented in Sec. 9.

2 Dispersion Equation for 1D Case

Below, we consider longitudinal vibrations of a multicomponent rod (see Fig. 1). The equations of motion of the neighboring rod parts follow [30]:

$$E_k u_{kxx} - \rho_k u_{ktt} = 0, \quad k = 1,2 \tag{1}$$

where E_k are the Young's moduli, ρ_k are the material densities, and u_k denotes the displacements ($k=1,2$).

On the contact surfaces, the following boundary conditions should be satisfied:

$$u_1 = u_2, \quad E_1 u_{1x} = E_2 u_{2x} \text{ for } x = 0 \tag{2}$$

Besides, the following quasi-periodicity condition is applied:

$$u_k(x+d,t) = u_k(x,t)\exp(ird) \tag{3}$$

where $k=1$, 2, and r denotes the quasi-momentum (wave number).

In particular, one obtains

$$u_k(d,t) = u_k(0,t)\exp(ird), \quad k = 1,2 \tag{4}$$

Solutions on rod parts are sought in the following form:

$$u_k(x,t) = A_k \exp[i(p_k x + \omega t)] + B_k \exp[i(-p_k x + \omega t)] \tag{5}$$

where $p_k=\omega/C_k$, $C_k=\sqrt{E_k/\rho_k}$, and $k=1,2$.

Substituting Eq. (5) into Eqs. (2) and (4), a system of four linear homogeneous algebraic equations regarding coefficients A_k and B_k is obtained. The system determinant gives the following transcendental dispersion equation:

$$\cos rd = \cos\Omega\cos(\Omega\tau) - \frac{\xi^2+1}{2\xi}\sin\Omega\sin(\Omega\tau) \tag{6}$$

where $\Omega=\omega L_1/C_1$, $\tau=L_2C_1/L_1C_2$, $\xi=\sqrt{E_1\rho_1}/\sqrt{E_2\rho_2}$, ω is the frequency, $r=2\pi/\lambda$ is the effective wave number, and λ is the wavelength [7].

In Eq. (6), parameter ξ represents the relative impedance of the composite and parameter τ represents the ratio of the times taken by a wave to cross the layers of the composite. It is clear that one may consider only interval $0\le\tau\le1$; otherwise, we can appropriately change the numeration of the composite layers.

If the frequency falls within a stop-band, the wave number becomes complex. In this case, the amplitude of the global wave is attenuated exponentially so no propagation is possible. The boundaries of the stop-bands are determined by equating the group velocity to zero, i.e., $d\omega/dr=0$. Equation (6) gives the following result for the boundary of the first stop-band:

$$\Omega = \pi/(1+\tau) \tag{7}$$

3 Long-Wave Asymptotics and Stop-Band for 1D Case

The derived transcendental dispersion Eq. (6) is further used for a detailed analysis of the solutions to the stated problem including the system fundamental singularities. However, this approach is impossible in the 2D case since a similar equation does not exist. This remark has an influence on the averaging process. Namely, having in mind Eq. (6), there is no need to construct an averaged equation directly from the boundary value problems (1)–(3). On the contrary, dispersion Eq. (6) for small Ω and small r directly yields the following relation:

$$\Omega = rd\left[(1+\tau)^2 + \frac{(\xi-1)^2\tau}{\xi}\right]^{-1/2} \tag{8}$$

It should be mentioned that for the particular case $\tau=1$ (physically, it means that time instants of wave propagation through neighboring rod parts are equal), Eq. (6) can be written as follows:

$$\cos rd = \cos^2\Omega - \frac{\xi^2+1}{2\xi}\sin^2\Omega \tag{9}$$

and hence one gets

$$\Omega = \pi k + \frac{rd\sqrt{\xi}}{\xi+1}, \quad k = 0, \pm1, \pm2, \ldots \tag{10}$$

Observe that from exact dispersion Eq. (6), one can obtain, arbitrarily, many terms of the homogenized solution. Consequently, a higher-order homogenization problem is analyzed further.

Since $0\le\tau\le1$, the application of the homogenization approach depends on the relative impedance of composite ξ. Owing to formula (8), it is evident that in the case of large values of ξ, the homogenization approach allows us only to estimate properly frequencies $\Omega\sim\sqrt{1/\xi}$.

The following frequency series is applied:

$$\omega^2 = \omega_0^2(1 + \varepsilon^2\omega_1 + \varepsilon^4\omega_2 + \varepsilon^6\omega_3 + \cdots) \tag{11}$$

where $\varepsilon=d/\lambda$ and $\omega_0\sim\varepsilon$.

We substitute Eq. (11) into the right-hand side of Eq. (5), develop both parts of Eq. (5) into a series regarding ε, and compare the coefficients standing by ε^{2i}, and we find ω_i, $i=1,2,3,\ldots$ (Appendix). A numerical example has been computed for the follow-

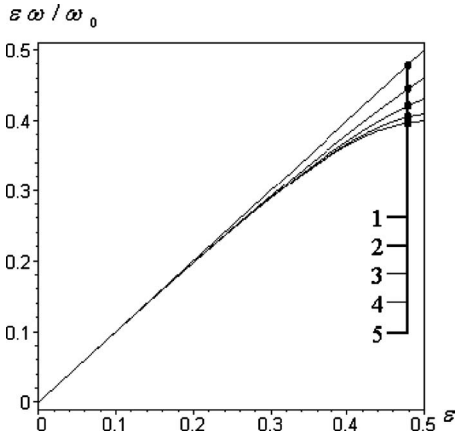

Fig. 2 Dispersion curves in the first pass band for the steel-aluminum 1D composite

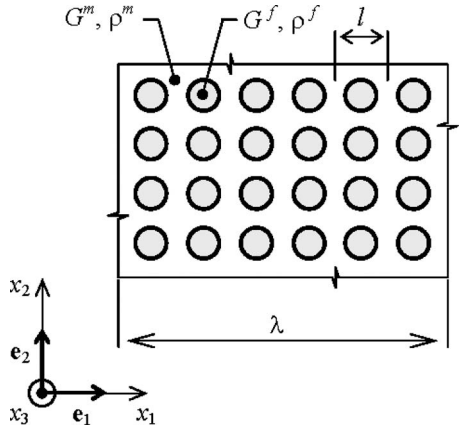

Fig. 3 Composite structure under consideration (*l* is the size of the unit cell and λ is the wavelength of the traveling signal)

ing two components: (1) steel, $E_1=210$ GPa, $\rho_1=7800$ kg/m^3, and $\alpha=0.3$ and (2) aluminum, $E_2=70$ GPa and $\rho_2=2700$ kg/m^3. In Fig. 2, acoustic modes of dispersion curves (within intervals of the first transmitting zone) are constructed according to the following formulas: (1) series Eq. (11) with the accuracy of $O(\varepsilon^0)$ (it corresponds to the quasi-homogeneous case), (2) series Eq. (11) with the accuracy of $O(\varepsilon^2)$, (3) series Eq. (11) with the accuracy of $O(\varepsilon^4)$, (4) series Eq. (11) with the accuracy of $O(\varepsilon^6)$, and (5) an exact solution to dispersion Eq. (6).

4 Asymptotics Regarding Relative Impedance

The governing Eq. (6) contains parameters ξ and τ, which enable the construction of alternative asymptotic solutions beside those via the homogenization approach. It should be emphasized that for $\xi=1$, an exact solution of Eq. (6) can be obtained. Furthermore, if $\xi=1+\varepsilon_1$ and $\varepsilon_1 \ll 1$, then

$$\cos rd = \cos[\Omega(1+\tau)] - \delta \sin\Omega \sin(\Omega\tau) \tag{12}$$

where $\delta=\varepsilon_1^2/2(1+\varepsilon_1) \ll 1$.

Zeroth approximation of the averaging procedure yields

$$\cos rd = \cos[\Omega_0(1+\tau)]$$

and hence

$$\Omega_0 = (rd + 2\pi k)/(1+\tau), \quad k = 0, \pm 1, \pm 2, \ldots$$

Assuming that

$$\Omega = \Omega_0 + \delta\Omega_1 + \cdots \tag{13}$$

and substituting Eq. (13) in Eq. (12) after a routine transformation, one obtains

$$\Omega_1 = -\frac{\sin\Omega_0 \sin(\Omega_0\tau)}{(1+\tau)\sin(rd)}$$

If $\xi \ll 1$, small parameter $\varepsilon_2=1/\xi$ can be introduced and a solution to Eq. (6) has the following form:

$$\varepsilon_2 \cos rd = \varepsilon_2 \cos\Omega \cos(\Omega\tau) - \tfrac{1}{2}(1+\varepsilon_2^2)\sin\Omega \sin(\Omega\tau) \tag{14}$$

The possible simplifications of Eq. (14) depend on an order of the quantity τ. For instance, if $\tau \sim 1$, i.e., $L_1/L_2 \sim \varepsilon_2$, then a solution to Eq. (13) can have the following form:

$$\Omega = \sqrt{\varepsilon_2}\Omega_0 + \varepsilon_2\Omega_1 + \cdots \tag{15}$$

Substituting series Eq. (15) into Eq. (14) gives the following first approximation:

$$\cos rd = 1 - \frac{1}{2\varepsilon_2}\sin(\sqrt{\varepsilon_2}\Omega_0)\sin(\sqrt{\varepsilon_2}\Omega_0\tau) \tag{16}$$

Development of the right-hand side of expression (16) into a series regarding Ω_0 and keeping the terms of the second and fourth orders enables approximation of the investigated system by a 1D periodic array of particles of two different types coupled by springs [14] with a relatively high accuracy.

On the other hand, if $\tau \sim \varepsilon_2$, i.e., $L_1/L_2 \sim 1$, a solution to Eq. (14) can have the following form:

$$\Omega = \Omega^{(0)} + \varepsilon_2\Omega^{(1)} + \cdots \tag{17}$$

Substituting series Eq. (17) into Eq. (14) gives the following first-order approximation:

$$\cos rd = \cos\Omega^{(0)} - 0.5\ \Omega^{(0)}\tau \sin\Omega^{(0)}$$

Therefore, an analysis of the 1D problem indicates that one may obtain an analytical solution to the stated problem, assuming that the characteristics of the occurring components strongly differ from each other and a small component exhibits the so-called small volume fracture.

5 Analysis of 2D Problem

Now, let us consider antiplane elastic shear waves propagating in the transverse x_1 and x_2 planes through a spatially infinite periodic composite material, which consists of an infinite matrix Ω^m and a square lattice of cylindrical fibers Ω^f (Fig. 3).

The governing wave equation has the following form:

$$\nabla_x \cdot (G\nabla_x u) = \rho\frac{\partial^2 u}{\partial t^2} \tag{18}$$

where G and ρ are the shear modulus and mass density, respectively, u is the displacement in the x_3 direction, $\nabla_x=\mathbf{e}_1\partial/\partial x_1 + \mathbf{e}_2\partial/\partial x_2$, and $\mathbf{e}_1$ and $\mathbf{e}_2$ are the unit Cartesian vectors.

Due to the heterogeneity of the composite medium, physical properties G and ρ are represented by piecewise continuous functions of coordinates, i.e.,

$$G(\mathbf{x}) = \begin{cases} G^m & \text{for } \mathbf{x} \in \Omega^m \\ G^f & \text{for } \mathbf{x} \in \Omega^f \end{cases}, \quad \rho(\mathbf{x}) = \begin{cases} \rho^m & \text{for } \mathbf{x} \in \Omega^m \\ \rho^f & \text{for } \mathbf{x} \in \Omega^f \end{cases} \tag{19}$$

where $\mathbf{x}=x_1\mathbf{e}_1+x_2\mathbf{e}_2$.

Taking into account representation Eq. (19), the input wave Eq. (18) can be written as follows:

$$G^a\nabla_{xx}^2 u = \rho^a\frac{\partial^2 u}{\partial t^2} \tag{20}$$

where G^a and ρ^a display the physical properties of the components and $\nabla_{xx}^2=\partial^2/\partial x_1^2+\partial^2/\partial x_2^2$. Here and in the sequel variables indexed by m correspond to the matrix, these indexed by f corre-

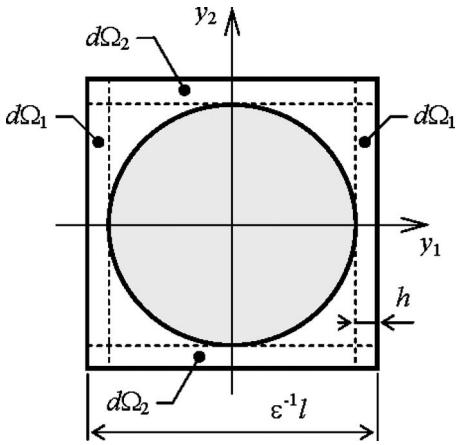

Fig. 4 A periodically repeated unit cell

spond to the fibers while index a takes both of these references $a=m$ and f. Equation (20) has to be accompanied by the perfect bonding conditions at the interface $\partial\Omega$ of the components, implying equalities of the displacement,

$$u^m = u^f \quad \text{on} \quad \partial\Omega \tag{21}$$

and of the tangential stress across the interface

$$G^m \frac{\partial u^m}{\partial \mathbf{n}} = G^f \frac{\partial u^f}{\partial \mathbf{n}} \quad \text{on} \quad \partial\Omega \tag{22}$$

where $\partial/\partial\mathbf{n}$ is the normal derivative to $\partial\Omega$.

6 Higher-Order AHM for 2D Problem

We start with the analysis of the dynamic BVPs (19)–(21) by the AHM [8]. Let us define a natural small parameter

$$\varepsilon = l/\lambda \tag{23}$$

characterizing the rate of nonhomogeneity of the composite structure. Here, microscopic size l corresponds to the length of a periodically repeated unit cell (Fig. 4) while macroscopic size λ can be associated with the wavelength of the traveling signal. In order to separate the macro- and microscale components of the solution, we introduce the so-called *slow* $\mathbf{x}$ and *fast* $\mathbf{y}$ variables

$$\mathbf{x} = \mathbf{x}, \quad \mathbf{y} = \varepsilon^{-1}\mathbf{x} \tag{24}$$

where $\mathbf{y}=y_1\mathbf{e}_1+y_2\mathbf{e}_2$ and we search for the displacement field in the form of the following asymptotic expansion:

$$u^a = u_0(\mathbf{x}) + \varepsilon u_1^a(\mathbf{x},\mathbf{y}) + \varepsilon^2 u_2^a(\mathbf{x},\mathbf{y}) + \cdots \tag{25}$$

The first term u_0 of expansion Eq. (25) represents a homogeneous part of the solution; it changes slowly within the whole sample of the material and does not depend on fast coordinates. All other terms u_i^a, $i=1,2,3,\ldots$, describe local variations in the displacements on the scale of nonhomogeneities. The spatial periodicity of the medium induces the same periodicity for u_i^a with respect to the fast coordinate,

$$u_i^a(\mathbf{x},\mathbf{y}) = u_i^a(\mathbf{x},\mathbf{y}+\boldsymbol{\lambda}_p) \tag{26}$$

where $\boldsymbol{\lambda}_p=\varepsilon^{-1}\mathbf{l}_p$, $\mathbf{l}_p=p_1\mathbf{l}_1+p_2\mathbf{l}_2$, $p_1,p_2=0,\pm1,\pm2,\ldots$, $\mathbf{l}_1$ and $\mathbf{l}_2$ are the fundamental translation vectors of the square lattice $\mathbf{l}_1=l\mathbf{e}_1$ and $\mathbf{l}_2=l\mathbf{e}_2$. The differential operators are as follows:

$$\nabla_x = \nabla_x + \varepsilon^{-1}\nabla_y, \quad \nabla_{xx}^2 = \nabla_{xx}^2 + 2\varepsilon^{-1}\nabla_{xy}^2 + \varepsilon^{-2}\nabla_{yy}^2 \tag{27}$$

where $\nabla_y=\mathbf{e}_1\partial/\partial y_1+\mathbf{e}_2\partial/\partial y_2$, $\nabla_{xy}^2=\partial^2/(\partial x_1\partial y_1)+\partial^2/(\partial x_2\partial y_2)$, and $\nabla_{yy}^2=\partial^2/\partial y_1^2+\partial/\partial y_2^2$.

Substituting formulas (23)–(25) and (27) into the input BVPs (20)–(22) and splitting them with respect to ε, we come to a recurrent sequence of cell BVPs involving microscopic wave equations,

$$G^a(\nabla_{xx}^2 u_{i-2}^a + 2\nabla_{xy}^2 u_{i-1}^a + \nabla_{yy}^2 u_i^a) = \rho^a \frac{\partial^2 u_{i-2}^a}{\partial t^2} \tag{28}$$

where $i=1,2,3,\ldots$, $u_{i-1}^a=0$, and microscopic perfect bonding conditions,

$$u_i^m = u_i^f \quad \text{on} \quad \partial\Omega \tag{29}$$

$$G^m\left(\frac{\partial u_{i-1}^m}{\partial \mathbf{n}} + \frac{\partial u_i^m}{\partial \mathbf{k}}\right) = G^f\left(\frac{\partial u_{i-1}^f}{\partial \mathbf{n}} + \frac{\partial u_i^f}{\partial \mathbf{k}}\right) \quad \text{on} \quad \partial\Omega \tag{30}$$

where $\partial/\partial\mathbf{k}$ is the normal derivative to $\partial\Omega$ defined in fast variables and $\mathbf{k}$ is the normal vector to $\partial\Omega$ also defined in fast variables. Due to the periodicity condition Eq. (26), the BVPs (28)–(30) can be considered only within one periodically repeated unit cell (Fig. 4) of the composite structure.

Solution of the ith BVPs (26) and (28)–(30) allows us to evaluate the term u_i^a. Knowing u_i^a, we apply the homogenizing operator $\int\int_{\Omega_0^f}(\cdot)dy_1dy_2+\int\int_{\Omega_0^m}(\cdot)dy_1dy_2$ over the unit cell domain $\Omega_0=\Omega_0^f+\Omega_0^m$ to the $(i+1)$th Eq. (28). The term u_{i+1}^a is eliminated by means of Green theorem and condition Eq. (30), which imply

$$G^f\int\int_{\Omega_0^f}(\nabla_{xy}^2 u_i^f + \nabla_{yy}^2 u_{i+1}^f)dy_1dy_2 + G^m\int\int_{\Omega_0^m}(\nabla_{xy}^2 u_i^m + \nabla_{yy}^2 u_{i+1}^m)dy_1dy_2 = 0$$

As a result, the homogenized equation of the ε^{i-1} order is obtained,

$$G^f\int\int_{\Omega_0^f}(\nabla_{xx}^2 u_{i-1}^f + \nabla_{xy}^2 u_i^f)dy_1dy_2 + G^m\int\int_{\Omega_0^m}(\nabla_{xx}^2 u_{i-1}^m + \nabla_{xy}^2 u_i^m)dy_1dy_2 = \rho^f\int\int_{\Omega_0^f}\frac{\partial^2 u_{i-1}^f}{\partial t^2}dy_1dy_2 + \rho^m\int\int_{\Omega_0^m}\frac{\partial^2 u_{i-1}^m}{\partial t^2}dy_1dy_2 \tag{31}$$

Combining the homogenized Eq. (31) at $i=1,2,3$, we determine the macroscopic wave equation of the order ε^2 in the following form:

$$\langle G\rangle_0\nabla_{xx}^2 u_0 + \varepsilon^2\lambda^2\langle G\rangle_2\nabla_1^4 u_0 + O(\varepsilon^4) = \langle\rho\rangle\frac{\partial^2 u_0}{\partial t^2} \tag{32}$$

where $\langle G\rangle_0$ is the effective shear modulus in the quasi-static case, coefficient $\langle G\rangle_2$ can be treated as the effective shear modulus of the order ε^2, $\langle\rho\rangle=(1-\varphi)\rho^m+\varphi\rho^f$ is the homogenized mass density, φ is the volume fraction of fibers, $0\le\varphi\le\pi/4$, and $\nabla_1^4=\partial^4/\partial x_1^4+\partial^4/\partial x_2^4$. Modules $\langle G\rangle_0$ and $\langle G\rangle_2$ are evaluated by the calculation of the integrals in formula (31). This was performed numerically in the program package MAPLE using standard in-built subroutines.

A solution of the cell problems presents one of the main difficulties in practical applications of the AHM. Owing to the obtained results regarding the 1D case, we develop an approximate asymptotic solution of BVPs (26) and (28)–(30) using as a natural small parameter, the nondimensional distance $\delta=2h/\lambda$ between the neighboring fibers. Let us suppose that $\delta\ll1$ and $G^f/G^m>1$. The length scales of thin matrix strips $d\Omega_1$ and $d\Omega_2$ in directions y_1 and y_2 are essentially different so the following first approximations are assumed:

$$\frac{\partial^2 u_i^m}{\partial y_1^2} \gg \frac{\partial^2 u_i^m}{\partial y_2^2} \quad \text{in the strip } d\Omega_1,$$

$$\frac{\partial^2 u_i^m}{\partial y_1^2} \ll \frac{\partial^2 u_i^m}{\partial y_2^2} \quad \text{in the strip } d\Omega_2 \tag{33}$$

Estimations of Eq. (33) are similar to the lubrication theory approach (see Ref. [31] for more details) because solutions in thin layers are changed in "thin" directions faster than normal to it.

The estimations allow us to simplify the cell BVPs and to derive approximate expressions for u_i^a in a closed analytical form. It should be noted that estimations of Eq. (33) and, therefore, the simplified solutions of the cell BVPs are obtained under assumptions of high contrast densely packed composites. However, numerical results for the effective modulus $\langle G\rangle_0$ practically show acceptable accuracy at all values of the volume fractions and properties of the components.

The second term appearing on the left-hand side of Eq. (32) predicts the effect of dispersion caused by the scattering of the global wave at the local heterogeneities of the composite medium. Let us consider a harmonic wave,

$$u_0 = U\exp(-i\mu x_s)\exp(i\omega t) \tag{34}$$

propagating parallel to axis x_s, $s=1,2$ with amplitude U, frequency ω, and wave number $\mu=2\pi/\lambda$. Substituting expression (34) into wave Eq. (32), we obtain the dispersion relation

$$\omega^2 = \omega_0^2\left[1 - 4\pi^2\frac{\langle G\rangle_2}{\langle G\rangle_0}\varepsilon^2 + O(\varepsilon^4)\right] \tag{35}$$

where $\omega_0=\mu v_0$ is the frequency and $v_0=\sqrt{\langle G\rangle_0/\langle\rho\rangle}$ is the wave velocity in the quasi-static case. Phase v_p and group v_g velocities follow:

$$v_p^2 = \left(\frac{\omega}{\mu}\right)^2 = v_0^2\left[1 - 4\pi^2\varepsilon^2\frac{\langle G\rangle_2}{\langle G\rangle_0} + O(\varepsilon^4)\right] \tag{36}$$

$$v_g^2 = \left(\frac{d\omega}{d\mu}\right)^2 = v_0^2\left[\frac{(1 - 8\pi^2\varepsilon^2\langle G\rangle_2/\langle G\rangle_0)^2}{1 - 4\pi^2\varepsilon^2\langle G\rangle_2/\langle G\rangle_0} + O(\varepsilon^4)\right] \tag{37}$$

The obtained asymptotic solutions (35)–(37) represent the long-wave approach, assuming that the wavelength λ is relatively large in comparison to the size of heterogeneity l of the composite structure.

7 PW Expansion Method and 2D Problem

In order to explore the high frequency range and to develop a solution valid for short waves, we study the input wave Eq. (18) by the PW expansion method [9,13]. According to the Floquet–Bloch theorem [5,6], a harmonic wave propagating through the heterogeneous composite material can be presented in the form

$$u = F(\mathbf{x})\exp(i\boldsymbol{\mu}\cdot\mathbf{x})\exp(i\omega t) \tag{38}$$

where $\boldsymbol{\mu}$ is the wave vector, $\boldsymbol{\mu}=\mu_1\mathbf{e}_1+\mu_2\mathbf{e}_2$, $F(\mathbf{x})$ is the modulation function with the aim to describe the influence of spatial periodicity of the medium, and $F(\mathbf{x})=F(\mathbf{x}+\mathbf{l}_p)$.

Let us expand function $F(\mathbf{x})$ and material properties $G(\mathbf{x})$ and $\rho(\mathbf{x})$ in terms of the infinite Fourier series

$$F(\mathbf{x}) = \sum_{k_1=-\infty}^{\infty}\sum_{k_2=-\infty}^{\infty} A_{k_1k_2}\exp\left[i\frac{2\pi}{l}(k_1x_1 + k_2x_2)\right]$$

$$G(\mathbf{x}) = \sum_{k_1=-\infty}^{\infty}\sum_{k_2=-\infty}^{\infty} B_{k_1k_2}\exp\left[i\frac{2\pi}{l}(k_1x_1 + k_2x_2)\right]$$

$$\rho(\mathbf{x}) = \sum_{k_1=-\infty}^{\infty}\sum_{k_2=-\infty}^{\infty} C_{k_1k_2}\exp\left[i\frac{2\pi}{l}(k_1x_1 + k_2x_2)\right] \tag{39}$$

where

$$B_{k_1k_2} = \frac{1}{l^2}\int\int_{\Omega_0} G(\mathbf{x})\exp\left[-i\frac{2\pi}{l}(k_1x_1 + k_2x_2)\right]dx_1dx_2$$

$$C_{k_1k_2} = \frac{1}{l^2}\int\int_{\Omega_0} \rho(\mathbf{x})\exp\left[-i\frac{2\pi}{l}(k_1x_1 + k_2x_2)\right]dx_1dx_2$$

Substituting Eq. (38) and expansion Eq. (39) into the wave Eq. (18) and collecting terms $\exp[i2\pi l^{-1}(j_1x_1+j_2x_2)]$ and $j_1,j_2=0,\pm1,\pm2,\ldots$, we come to an infinite system of linear algebraic equations for the unknown coefficient $A_{k_1k_2}$,

$$\sum_{k_1=-\infty}^{\infty}\sum_{k_2=-\infty}^{\infty} A_{k_1k_2}\left\{B_{\substack{j_1-k_1,\\ j_2-k_2}}\left[\left(\frac{2\pi}{l}k_1+\mu_1\right)\left(\frac{2\pi}{l}j_1+\mu_1\right) + \left(\frac{2\pi}{l}k_2+\mu_2\right)\left(\frac{2\pi}{l}j_2+\mu_2\right)\right] - C_{\substack{j_1-k_1,\\ j_2-k_2}}\omega^2\right\} = 0 \tag{40}$$

System of linear algebraic Eq. (40) has a nontrivial solution if and only if the determinant of the matrix of the coefficient $A_{k_1k_2}$ is zero. In the numerical examples presented below, the dispersion relations are calculated approximately by truncation of the infinite system (40) (and hence its corresponding infinite determinant), assuming that $-j_{\max}\le j_s\le j_{\max}$. The introduced truncation procedure allows us to study the finite determinant instead of the infinite one. The number of the kept equations is $n=2j_{\max}+1$. We expect that an increase in $j_{\max}$ shall improve the accuracy of the solution. From the physical point of view, such a truncation means cutting off higher frequencies. It should be noted that the PW expansion method does not use explicitly bonding condition Eqs. (21) and (22), whereas they are "embedded" implicitly into Eq. (18) and expansion Eq. (39).

To illustrate the occurrence of phononic band gaps, let us rewrite expression (38), separating real $\boldsymbol{\mu}_R$ and imaginary $\boldsymbol{\mu}_I$ parts of the wave vector $\boldsymbol{\mu}=\boldsymbol{\mu}_R+i\boldsymbol{\mu}_I$

$$u = F(\mathbf{x})\exp(-\boldsymbol{\mu}_I\cdot\mathbf{x})\exp(i\boldsymbol{\mu}_R\cdot\mathbf{x})\exp(i\omega t) \tag{41}$$

It can easily be seen that if the wave propagates at a frequency making the wave number complex, then the signal Eq. (41) attenuates exponentially; the imaginary part μ_I of the wave number represents the attenuation factor. Thus, the frequency bands where $\mu_I\neq0$ are called stop-bands, while the bands where $\mu_I=0$ are called the pass bands.

8 Numerical Examples and Discussion

As the first example, let us consider a low contrast composite consisting of nickel fibers ($G^f=75.4$ GPa, $\rho^f=8936$ kg/m^3, and $\varphi=0.35$) and an aluminum matrix ($G^m=27.9$ GPa and $\rho^f=2697$ kg/m^3). Figure 5 displays the dispersion curves within the first and the second pass bands calculated by the PW expansion method. The plot is divided into two (left and right) parts. The left part displays results for the diagonal OB, whereas the right part displays results for the directions of the wave propagation being orthogonal to OA. Results obtained at $j_{\max}=1$ and $j_{\max}=2$ are very close, which confirms the fast convergence of the procedure.

The qualitative behavior of the solution can be described as follows. At very low frequencies, the dispersion curve is almost straight $\omega\approx\omega_0$ and the phase and group velocities are nearly equal and independent of the frequency $v_p\approx v_g\approx v_0$, so the waves propagate in the composite medium as if it was homogeneous (this is a so-called quasi-static case).

As the frequency increases, the slope of the dispersion curve in the first pass band decreases. Both phase and group velocities

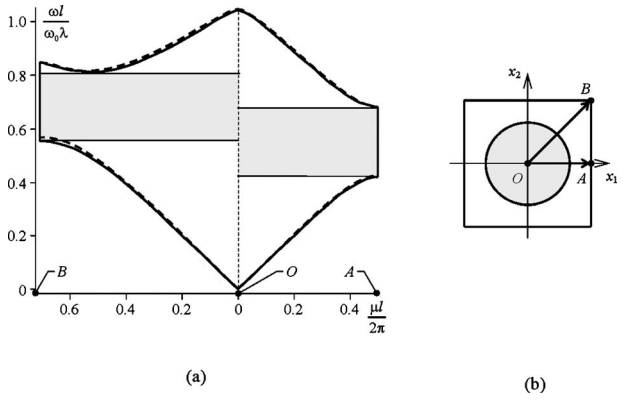

Fig. 5 (*a*) Phononic bands for the nickel-aluminum composite (dashed line: $j_{max}=1$ and solid line: $j_{max}=2$) and (*b*) directions of the wave vector μ

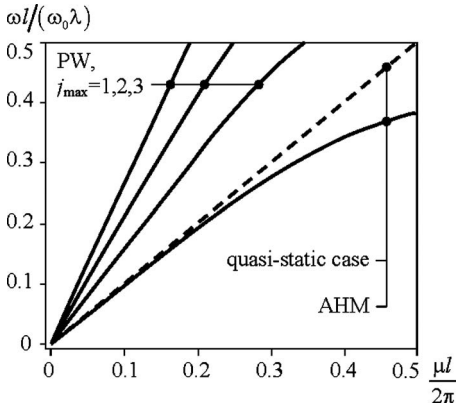

Fig. 7 Dispersion curves in the first pass band for the carbon-epoxy composite

decrease, but the group velocity decreases faster $v_p > v_g$. At the highest frequency in the first pass band, the dispersion curve has zero slope $v_g=0$, which corresponds to the case of a stationary wave. Within the stop-band (shaded area in Fig. 5), wave number μ is complex so the amplitude of the wave attenuates exponentially and no propagation is possible. In the second pass band, the group velocity varies from zero at the edges to a maximum value near the center. The dispersion curve is flatter than in the first pass band, which indicates lower values of the group velocity.

Figure 5 reveals that in the quasi-static case, the problem under consideration is isotropic. With the increase in frequency (and in the higher-order approximations of the AHM), we observe the anisotropic behavior of the 2D square lattice. This can easily be explained because the ratio of the wavelength to the distance between neighboring fibers depends on the direction of propagation. Hence, the phononic band structures in orthogonal *OA* and diagonal *OB* directions are different.

Figure 6 compares the dispersion curves in the first pass band calculated by the AHM and the PW expansion methods. We can observe that the AHM allows us to predict the dispersion phenomenon, but the accuracy of the obtained results is acceptable only at low frequencies.

As the second example, let us consider a high contrast composite consisting of carbon fibers ($G^f=86$ GPa, $\rho^f=1800$ kg/m^3, and $\varphi=0.5$) and an epoxy matrix ($G^m=1.53$ GPa and $\rho^m=1250$ kg/m^3). Figure 7 displays the dispersion curves calculated for the first pass band. It can be seen that the PW expansion method converges significantly worse than in the low contrast case; meanwhile, the AHM provides qualitatively correct results up to the beginning of the first stop-band.

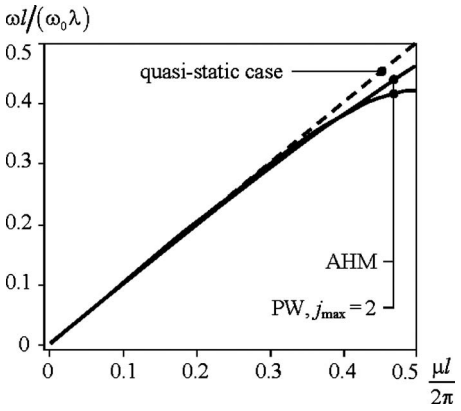

Fig. 6 Dispersion curves in the first pass band for the nickel-aluminum 2D composite

9 Concluding Remarks

The main conclusion of our research may be formulated as follows. The obtained asymptotic solutions for the 1D problem allow us to study the cases, where construction of an exact dispersion equation is impossible, for instance, in nonlinear cases or in linear 2D and 3D cases. Besides, the analysis of exact dispersion equation indicates that the homogenization procedure is only part of a wide spectrum of approximated methods. Namely, one may effectively apply asymptotic series regarding other parameters being suitable in investigation not only in low but also in higher frequency oscillation regions.

Let us have a deeper insight into this question. The following nondimensional parameters occur in the dispersion equation: r, $\tau=L_2C_1/(L_1C_2)$, and $\xi=\sqrt{E_1\rho_1/E_2\rho_2}$. Parameter r plays a key role in the averaging procedure. However, we have shown that there is also other limiting asymptotics not related to r, which can be applied for the arbitrary length of waves, for example, for $\tau=j$, where j is the integer; $\xi=1+\varepsilon$, $\varepsilon \ll 1$, and $\varepsilon_1=1/\xi$. Proceeding like in the 1D case, a similar expansion for 2D case can be found.

In the present paper, antiplane shear waves in a fiber-reinforced composite material with a square lattice of cylindrical fibers are also studied. Successive reflections and refractions of the signal at the interface of the components result in the formation of pass and stop frequency bands so the composite acts as a discrete wave filter. The application of a higher-order AHM provides a long-wave approach valid in the low frequency range. The solution for the high frequencies is obtained by the PW expansion method. However, this approach may run into convergence problems with the increase in contrast between properties of the components. Eventually, we may conclude that the higher-order AHM and the PW expansion method can be treated as complementary to each other. The dispersion curves are obtained and the pass and stop-bands are identified.

Acknowledgment

This work has been supported by the German Research Foundation (Deutsche Forschungs Gemeinschaft) under Grant No. WE 736/25-1 for I.V.A. and D.W. and by the Alexander Von Humboldt Foundation (Institutional Academic Co-operation Program) under Grant No. 3.4-Fokoop-UKR/1070297 for I.V.A., V.V.D., and D.W.

Appendix

Expressions of ω_1, ω_2, and ω_3 are obtained using MAPLE and the following notation is applied: $E1 \equiv E_1$, $E2 \equiv E_2$, $\rho 1 \equiv \rho_1$, $\rho 2 \equiv \rho_2$, and $\alpha = L_1/d$,

$$\omega 1 := -\frac{\pi^2(-E1\rho 1 + E2\rho 2)^2(\alpha-1)^2\alpha^2}{3((E1-E2)\alpha - E1)^2((\rho 2-\rho 1)\alpha-\rho 2)^2}$$

$$\omega 2 := -4\pi^4(-E1\rho 1 + E2\rho 2)^2\left(\left(\left(-3E1E2 - \frac{1}{2}E2^2 + E1^2\right)\rho 2^2 - 3\rho 1\left(\frac{11}{3}E1E2 + E1^2 + E2^2\right)\rho 2 - \frac{\rho 1^2(-2E2^2 + 6E1E2 + E1^2)}{2}\right)\alpha^4 + ((9E1E2 - 4E1^2 + E2^2)\rho 2^2 + (9E1^2\rho 1 + 3\rho 1E2^2 - 22E1E2\rho 1)\rho 2 + \rho 1^2E1(E1 + 3E2))\alpha^3 + \left(\left(-\frac{1}{2}E2^2 + 6E1^2 - 9E1E2\right)\rho 2^2 - 9\left(-\frac{11E2}{9} + E1\right)\rho 1E1\rho 2 - \frac{E1^2\rho 1^2}{2}\right)\alpha^2 + ((3E1E2 - 4E1^2)\rho 2^2 + 3\rho 2E1^2\rho 1)\alpha + \rho 2^2E1^2\right)(\alpha-1)^2\alpha^2/(45((\rho 2-\rho 1)\alpha-\rho 2)^4((E1 - E2)\alpha - E1)^4)$$

$$\omega 3 := -32\pi^6\alpha^2(\alpha-1)^2\left(\left(\left(\left(E1^4 + 6E1^2E2^2 + \frac{3}{32}E2^4 + \frac{27}{8}E1E2^3 - 5E1^3E2\right)\rho 2^4 - 5\left(-\frac{59}{10}E1^3E2 - \frac{27}{40}E2^4 + \frac{79}{8}E1^2E2^2 + \frac{3}{40}E1E2^3 + E1^4\right)\rho 1\rho 2^3 + 6\left(-\frac{395}{48}E1^3E2 + \frac{1913}{96}E1^2E2^2 - \frac{395}{48}E1E2^3 + E2^4 + E1^4\right)\rho 1^2\rho 2^2 + \frac{27\left(-\frac{40}{27}E2^4 + E1^4 - \frac{395}{27}E1^2E2^2 - \frac{1}{9}E1^3E2 + \frac{236}{27}E1E2^3\right)\rho 1^3\rho 2}{8} + \frac{3\left(\frac{32}{3}E2^4 + E1^4 + 64E1^2E2^2 + 36E1^3E2 - \frac{160}{3}E1E2^3\right)\rho 1^4}{32}\right)\alpha^8 + \left(\left(-8E1^4 - 36E1^2E2^2 - \frac{3}{8}E2^4 + 35E1^3E2 - \frac{135}{8}E1E2^3\right)\rho 2^4 + 35\rho 1\left(\frac{395}{56}E1^2E2^2 - \frac{81}{280}E2^4 - \frac{177}{35}E1^3E2 + E1^4 + \frac{3}{70}E1E2^3\right)\rho 2^3 - 36\left(\frac{1913}{144}E1^2 - \frac{1975}{288}E1^3E2 + E1^3 + \frac{1}{4}E2^4 - \frac{395}{96}E1E2^3\right)\rho 1^2\rho 2^2 - \frac{135\rho 1^3\left(\frac{4}{45}E1^3E2 + E1^4 - \frac{8}{27}E2^4 - \frac{79}{9}E1^2E2^2 + \frac{472}{135}E1E2^3\right)\rho 2}{8} - \frac{3\left(-\frac{40}{3}E2^3 + 32E1E2^2 + 27E1^2E2 + E1^3\right)\rho 1^4E1}{8}\right)\alpha^7 + \left(\left(90E1^2E2^2 + 28E1^4 - 105E1^3E2 + \frac{9}{16}E2^4 + \frac{135}{4}E1E2^3\right)\rho 2^4 - 105\left(\frac{3}{140}E1E2^3 - \frac{59}{14}E1^3E2 - \frac{27}{280}E2^4 + E1^4 + \frac{395}{84}E1^2E2^2\right)\rho 1\rho 2^3 + 90\rho 1^2\left(E1^4 + \frac{1913}{240}E1^2E2^2 - \frac{395}{72}E1^3E2 + \frac{1}{15}E2^4 - \frac{79}{48}E1E2^3\right)\rho 2^2 + \frac{135\left(\frac{1}{15}E1^2E2 + E1^3 - \frac{79}{18}E1E2^2 + \frac{118}{135}E2^3\right)\rho 1^3E1\rho 2}{4} + \frac{9\left(E1^2 + 18E1E2 + \frac{32}{3}E2^2\right)\rho 1^4E1^2}{16}\right)\alpha^6 + \left(\left(-120E1^2E2^2 - \frac{3}{8}E2^4 - \frac{135}{4}E1E2^3 - 56E1^4 + 175E1^3E2\right)\rho 2^4 + 175\left(\frac{118}{35}E1^3E2 + E1^4 - \frac{27}{1400}E2^4 + \frac{3}{350}E1E2^3 + \frac{79}{28}E1^2E2^2\right)\rho 1\rho 2^3 - 120\rho 1^2\left(\frac{1913}{480}E1E2^2 - \frac{395}{96}E1^2E2 - \frac{79}{192}E2^3 + E1^3\right)E1\rho 2^2 - \frac{135\left(E1^2 - \frac{79}{54}E2^2 - \frac{2}{45}E1E2\right)\rho 1^3E1^2\rho 2}{4} - \frac{3\rho 1^4E1^3(E1 + 9E2)}{8}\right)\alpha^5 + \left(\left(-175E1^3E2 + 70E1^4 + \frac{135}{8}E1E2^3 + \frac{3}{32}E2^4 + 90E1^2E2^2\right)\rho 2^4 - 175\rho 1\left(\frac{79}{56}E1E2^2 - \frac{177}{70}E1^2E2 + E1^3 + \frac{3}{1400}E2^3\right)E1\rho 2^3 + 90\left(-\frac{395}{144}E1E2 + \frac{1913}{1440}E2^2 + E1^2\right)\rho 1^2E1^2\rho 2^2 + \frac{135\left(E1 - \frac{E2}{45}\right)\rho 1^3E1^3\rho 2}{8}$$

$$+\frac{3E1^4\rho1^4}{32}\Bigg)\alpha^4-56\Bigg(\Bigg(E1^3+\frac{27}{448}E2^3+\frac{9}{14}E1E2^2-\frac{15}{8}E1^2E2\Bigg)\rho2^3-\frac{15\rho1\Big(\frac{59}{35}E1E2+E1^2+\frac{79}{168}E2^2\Big)E1\rho2^2}{8}$$

$$+\frac{9\Big(-\frac{395E2}{288}+E1\Big)\rho1^2E1^2\rho2}{14}+\frac{27\rho1^3E1^3}{448}\Bigg)\rho2E1\alpha^3+\Bigg((6E1^2E2^2+28E1^4-35E1^3E2)\rho2^4-35\rho1\Big(-\frac{59E2}{70}+E1\Big)E1^3\rho2^3$$

$$+6\rho2^2E1^4\rho1^2\Bigg)\alpha^2+((5E1^3E2-8E1^4)\rho2^4+5\rho2^3E1^4\rho1)\alpha+\rho2^4E1^4\Bigg)(-E1\rho1+E2\rho2)^2/(945((\rho2-\rho1)\alpha-\rho2)^6((E1-E2)\alpha$$

$$-E1)^6)$$

References

[1] Bakhvalov, N. S., and Panasenko, G. P., 1989, *Homogenization: Averaging Processes in Periodic Media. Mathematical Problems in Mechanics of Composite Materials*, Kluwer, Dordrecht.

[2] Bensoussan, A., Lions, J.-L., and Papanicolaou, G., 1978, *Asymptotic Analysis for Periodic Structures*, North-Holland, Amsterdam.

[3] Bakhvalov, N. S., and Eglit, M. E., 2000, "Long-Wave Asymptotics With Dispersion for Wave Propagation in Stratified Media. I. Waves Orthogonal to the Layers," Russian J. Numerical Analysis and Mathematical Modelling, **15**(1), pp. 3–14.

[4] Bakhvalov, N. S., and Eglit, M. E., 2000, "Long-Wave Asymptotics With Dispersion for Wave Propagation in Stratified Media. II. Waves in Arbitrary Directions," Russian J. Numerical Analysis and Mathematical Modelling, **15**(3–4), pp. 225–236.

[5] Floquet, G., 1883, "Sur les équations différentielles linéaires à coefficients périodiques," Ann. Sci. Ec. Normale Super., Ser. 2, **12**, pp. 47–88.

[6] Bloch, F., 1928, "Über die Quantenmechanik der Elektronen in Kristallgittern," Z. Phys., **52**, pp. 555–600.

[7] Bedford, A., and Drumheller, D. S., 1994, *Introduction to Elastic Wave Propagation*, Wiley, New York.

[8] Boutin, C., and Auriault, J. L., 1993, "Rayleigh Scattering in Elastic Composite Materials," Int. J. Eng. Sci., **31**, pp. 1669–1689.

[9] Kushwaha, M. S., Halevi, P., Martinez, G., Dobrzynski, L., and Djafari-Rouhani, B., 1994, "Theory of Acoustic Band Structure of Periodic Elastic Composites," Phys. Rev. B, **49**, pp. 2313–2322.

[10] Tanaka, Y., Tomoyasu, Y., and Tamura, S.-I., 2000, "Band Structure of Acoustic Waves in Phononic Lattices: Two-Dimensional Composites With Large Acoustic Mismatch," Phys. Rev. B, **62**, pp. 7387–7392.

[11] Sigalas, M. M., and Economou, E. N., 1992, "Elastic and Acoustic Wave Band Structure," J. Sound Vib., **158**(2), pp. 377–382.

[12] Sigalas, M. M., and Economou, E. N., 1993, "Band Structure of Elastic Waves in Two Dimensional Systems," Solid State Commun., **86**, pp. 141–143.

[13] Sigalas, M. M., Kushwaha, M. S., Economou, E. N., Kafesaki, M., Psarobas, I. E., and Steurer, W., 2005, "Classical Vibrational Modes in Phononic Lattices: Theory and Experiment," Z. Kristallogr., **220**(9–10), pp. 765–809.

[14] Movchan, A. B., Movchan, N. V., and Poulton, C. G., 2002, *Asymptotic Models of Fields in Dilute and Densely Packed Composites*, Imperial College, London.

[15] Kafesaki, M., and Economou, E. N., 1999, "Multiple-Scattering Theory for Three-Dimensional Periodic Acoustic Composites," Phys. Rev. B, **60**, pp. 11993–12001.

[16] Zhikov, V. V., 1989, "Spectral Approach to Asymptotic Diffusion Problems," Diff. Eq., **25**(1), pp. 33–39.

[17] Jikov, V. V., Kozlov, S. M., and Oleinik, O. A., 1994, *Homogenization of Differential Operators and Integral Functionals*, Springer-Verlag, Berlin.

[18] Allaire, G., and Conca, C., 1998, "Bloch Wave Homogenization and Spectral Asymptotic Analysis," J. Math. Pures Appl., **77**(2), pp. 153–208.

[19] Birman, M. S., and Suslina, T. A., 2004, "Periodic Second-Order Differential Operators. Threshold Properties and Averaging," St. Petersbg. Math. J., **15**(5), pp. 639–714.

[20] Zhikov, V. V., 2005, "On the Spectral Method in Homogenization Theory," Proc. Steklov Inst. Math., **3**(250), pp. 85–94.

[21] Conca, C., Natesan, S., and Vanninathan, M., 2006, "Numerical Experiments With the Bloch–Floquet Approach in Homogenization," Int. J. Numer. Methods Eng., **65**(9), pp. 1444–1471.

[22] Smyshlyaev, V. P., and Cherednichenko, K. D., 2000, "On Rigorous Derivation of Strain Gradient Effects in the Overall Behaviour of Periodic Heterogeneous Media," J. Mech. Phys. Solids, **48**(6–7), pp. 1325–1357.

[23] Zhikov, V. V., 2005, "Gaps in the Spectrum of Some Elliptic Operators in Divergent Form With Periodic Coefficients," St. Petersbg. Math. J., **16**, pp. 773–790.

[24] Bouchitté, G., and Felbacq, D., 2004, "Homogenization Near Resonances and Artificial Magnetism From Dielectrics," C. R. Math. Acad. Sci., **339**(5), pp. 377–382.

[25] Bellieud, M., and Gruais, I., 2005, "Homogenization of an Elastic Material Reinforced by Very Stiff or Heavy Fibers. Non-Local Effects. Memory Effects," J. Math. Pures Appl., **84**, pp. 55–96.

[26] Babych, N. O., Kamotski, I. V., and Smyshlyaev, V. P., 2008, "Homogenization in Periodic Media With Doubly High Contrasts," Networks Heterog. Media, **3**(3), pp. 413–436.

[27] Ávila, A., Griso, G., Miara, B., and Rohan, E., 2008, "Multiscale Modeling of Elastic Waves: Theoretical Justification and Numerical Simulation of Band Gaps," Multiscale Model. Simul., **7**(1), pp. 1–21.

[28] Smyshlyaev, V. P., 2009, "Propagation and Localization of Elastic Waves in Highly Anisotropic Composites via Homogenization," Mech. Mater., **41**, pp. 434–447.

[29] Cao, Y., Hou, Z., and Liu, Y., 2004, "Finite Difference Time Domain Method for Band-Structure Calculations of Two-Dimensional Phononic Crystals," Solid State Commun., **132**(8), pp. 539–543.

[30] Chen, W., and Fish, J., 2001, "A Dispersive Model for Wave Propagation in Periodic Heterogeneous Media Based on Homogenization With Multiple Spatial and Temporal Scales," ASME J. Appl. Mech., **68**, pp. 153–161.

[31] Tayler, A. B., 2001, *Mathematical Models in Applied Mechanics*, Oxford University Press, Oxford.